



# Modelling the downstream longitudinal effects of frequent hydropeaking on the spawning potential and stranding susceptibility of salmonids



Anton J. Burman<sup>a,\*</sup>, Richard D. Hedger<sup>b</sup>, J. Gunnar I. Hellström<sup>a</sup>, Anders G. Andersson<sup>a</sup>, Line E. Sundt-Hansen<sup>b</sup>

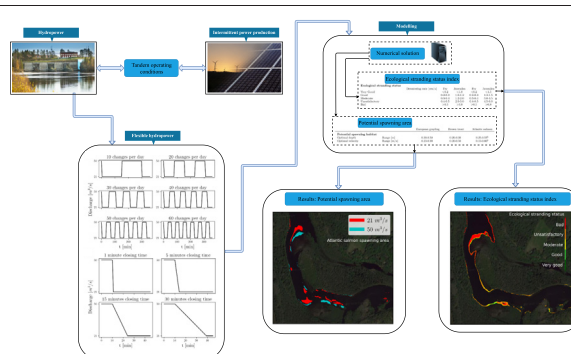
<sup>a</sup> Division of Fluid and Experimental Mechanics, Department of Engineering Sciences and Mathematics, Luleå University of Technology, 971 87 Luleå, Sweden

<sup>b</sup> Norwegian Institute for Nature Research – NINA, NO-7034 Trondheim, Norway

## HIGHLIGHTS

- Hydrodynamic scenarios with very high hydropeaking frequencies were modeled.
- A general method of computing dewatering time for any numerical model was provided.
- Higher hydropeaking frequencies had smaller amounts of potential spawning areas.
- High frequencies lowered the portion of potential spawning area at risk of dewatering.

## GRAPHICAL ABSTRACT



## ARTICLE INFO

### Article history:

Received 2 June 2021

Received in revised form 8 July 2021

Accepted 8 July 2021

Available online 14 July 2021

Editor: Fernando A.L. Pacheco

### Keywords:

Hydropeaking  
Spawning habitat  
Salmonids  
Modelling  
Dewatering

## ABSTRACT

Hydropower plant operating conditions are expected to change to be more in tandem with intermittent power production so as to meet the requirements of the Paris Agreement, which in turn may negatively impact ecological conditions downstream of the hydropower plants. The current study investigates how highly flexible hydropower operating conditions may impact several salmonid species (European grayling, Atlantic salmon and brown trout) in the River Umeälven, a major river in northern Sweden; specifically, how changes in hydropeaking frequency may affect the area of the downstream watercourse that is hydraulically suitable for spawning (potential spawning area) and how changes in spill gate closing time may affect the propensity to stranding. River hydrodynamics were modeled using the open-source solver Delft3D, with a range of hydropeaking frequencies (from 10 to 60 starts and stops per day) and a range of spill gate closing times from (1–30 min). Increasing the hydropeaking frequency caused a reduction in potential spawning area, but also a reduction in dewatering of potential spawning area at low flows. Increasing spill gate closing time caused a decrease in propensity to stranding. Effects were dependent on both species and life-stage, and declined longitudinally with distance downstream from the spillway outlet. The modelling approach used here provides an effective method for predicting likely outcomes of flexible hydropower operating conditions, taking into account fish species and life-stages present and watercourse characteristics.

© 2021 The Authors. Published by Elsevier B.V. This is an open access article under the CC BY license (<http://creativecommons.org/licenses/by/4.0/>).

## 1. Introduction

To fulfill goals set in the Paris Agreement (UNFCCC, 2016), increased dependence on intermittent power production from solar-, wind- and wave-power is expected in the coming years. Consequent changes may therefore be required in the operating conditions of current

\* Corresponding author.

E-mail address: [anton.burman@ltu.se](mailto:anton.burman@ltu.se) (A.J. Burman).

hydropower plants so that they operate more in tandem with intermittent power production requirements, and future operating conditions may require increased flexibility (HydroFlex, 2020) to account for larger shifts in local weather conditions. This flexibility may necessitate increased occurrence of hydropeaking and hydrofibrillation in watercourses. Hydropeaking, the discontinuous release of water from a storage basin to generate energy to satisfy peaks in demand, causes rapid changes in water level downstream of turbines, causing either rapid up- or down-ramping of the turbines (Moreira et al., 2019). Hydrofibrillation may also be initiated in run-of-the-river power plants, resulting in flow fluctuations of similar frequency to those of hydropeaking but with smaller magnitude (Greimel et al., 2015).

Hydropeaking may have significant effects on watercourses. Increases in velocities and bottom shear stress related to rapidly fluctuating discharge may increase suspended sediment, which in turn can deplete the downstream reach of fine sediments (Vericat et al., 2020). Additionally, rapid flow fluctuations can reduce riverbank stability (Mohammed-Ali et al., 2020). Hydropeaking may negatively impact fish populations (McKinney et al., 2001) by altering spawning behavior (Vollset et al., 2016), reducing body growth (Flodmark et al., 2004; Puffer et al., 2017), and delaying the timing of the smolt run (Bakken et al., 2016b). Dewatering during low flows in the hydropeaking cycle may cause mortality due to egg desiccation in dewatered redds (Casas-Mulet et al., 2015; Bakken et al., 2016a) and suffocation of juveniles stranded in dewatered areas (Saltveit et al., 2001, 2020). A sharp decrease in discharge causes rapid dewatering of beach zones which is associated with stranding and entrapment of salmonids (Saltveit et al., 2001; Halleraker et al., 2003), and may be a critical problem for fry and juveniles (Moreira et al., 2019) which have limited dispersive ability. Effects of dewatering are species-specific (Saltveit et al., 2001; Halleraker et al., 2003) and depend on species interactions. In rivers where brown trout (*Salmo trutta*) coexist with Atlantic salmon (*Salmo salar*), brown trout tend to reside closer to the river banks compared to rivers when they are the only salmonid species present (Bremset and Berg, 1999; Bremset and Heggenes, 2001; Berg et al., 2014), and are especially exposed to rapid dewatering of beaches.

Physical habitat simulation modelling may be used as an investigative and predictive tool for modelling the spatial distribution of fish within rivers with respect to habitat characteristics. This approach has previously been applied to model potential spawning habitats, both in Atlantic salmon in the River Dee, Scotland (Moir et al., 2005) and in chinook salmon (*Oncorhynchus tshawytscha*) in the Merced River and the Lower American rivers in California, USA (Gallagher and Gard, 1999). Research on instream flow-velocity and flow-depth requirement necessary for salmonid spawning (e.g. Louhi et al., 2008; Gónczi, 1989) may be integrated with hydrodynamic modelling to predict how hydropeaking regimes may influence the available habitat with suitable flow conditions for spawning. Likewise, research on flow condition requirements for fry and juveniles may be integrated with hydrodynamic modelling to determine parts of the watercourse susceptible to stranding.

The research consortium HydroFlex (HydroFlex, 2020) was created to provide scientific and technological breakthroughs enabling hydropower to operate with very high flexibility to utilize the full power and storage capability. One of the goals was to investigate and mitigate the potential environmental impact due to increased hydropeaking frequency, involving multiple hydropeaking events per day. The impact of very high frequent hydropeaking on the spawning habitats downstream reach is at the time of writing this paper, not well understood. Increasing the frequency of hydropeaking affects downstream reaches by directly impacting the amplitude and frequency of variation in downstream discharge, but also constrains the spill gate closing time (high frequencies necessitate short closing times) to also affect the rate of change of discharge. In this study, a general modelling approach was developed to assess potential impacts of highly flexible hydropower operating conditions on selected salmonid fish species. Information on optimal flow conditions for several species and two stages (fry

and juveniles) of salmonids provided from literature was combined with hydraulic predictions of flow conditions in a watercourse subjected to hydropeaking, to determine how flexible operating conditions, involving changes in hydropeaking frequency and spill gate closing time, could affect the total area that was hydraulically suitable for spawning (defined here as potential spawning area) and the likelihood of fish avoiding stranding in the bypass reach downstream of a hydropower dam.

## 2. Materials and methods

### 2.1. Study site

The study was carried out in the bypass reach of the Stornorrfor hydropower plant in the river Umeälven in northern Sweden (Fig. 1). Stornorrfor is the plant in Sweden with the highest annual electricity production (Vattenfall, 2020). The adjacent bypass reach is used for both spilling during flooding or turbine downtime and as a passage for upstream fish migration. In winter, the reach becomes nearly dewatered, potentially resulting in mortality of resident fish. During the summer the discharge usually varies between 21 m<sup>3</sup>/s and 50 m<sup>3</sup>/s. The discharge of 21 m<sup>3</sup>/s is equivalent to that through the fish ladder at the top of the bypass, which is used for fish migration past the dam in the summer. The discharge is then often increased to 50 m<sup>3</sup>/s for aesthetic reasons during weekends. The discharge from the spillways annually exceeds 1000 m<sup>3</sup>/s (Länsstyrelsen i Norrbotten, 2017).

Several fish species are present in the reach during summer. Freshwater species such as pike (*Esox lucius*) and perch (*Perca fluviatilis*) likely enter the reach via downstream displacement during spilling or downstream migration from tributaries. The reach is also used for upstream migration by salmonids such as brown trout and Atlantic salmon (Vattenfall, 2020), and the reach and its tributaries may also be used by spawning salmonids. In summer, three salmonid species reside in the reach; European grayling (*Thymallus thymallus*), brown trout and Atlantic salmon. Locally hatched juveniles are released annually into the reach to sustain the valuable fish populations in the protected, unregulated River Vindelälven, which confluences with the River Umeälven 10 km upstream of Stornorrfor (Vattenfall, 2020).

### 2.2. Modelling reach hydrodynamics

Reach hydrodynamics were modeled using the Delft3d modelling suite (Deltares, 2021). Reach bathymetry was created from a Digital Elevation Model derived from drone photogrammetry (accuracy ≈0.1 m) conducted during winter when the reach was mostly dewatered (Angele and Andersson, 2018) (Fig. 2a). The transient hydraulics of the river were solved in 2D using the Shallow Water Equations (SWE), which are derived from the fundamental Navier-Stokes equations by assuming hydrostatic pressure, and that the horizontal length scales are significantly larger than the vertical length scales (Cushman-Roisin and Beckers, 2011). The Manning number (see Fig. 2b) was calibrated for the steady state hydraulic simulations ( $Q=21$  m<sup>3</sup>/s and 50 m<sup>3</sup>/s) and dynamic hydraulic conditions were validated (Burman et al., 2019, 2020) using measurements of water level made with eight pressure sensors in the reach in summer 2017 (placements shown in Fig. 1). Delft3D uses curvi-linear finite differences for the spatial discretization and an alternating-direction-implicit (ADI) method for the integration in time (Deltares, 2014). A previous study (Burman et al., 2020) concluded that a mesh of approximately 453,000 nodes was sufficient to resolve the reach. The model requires three boundary conditions; one upstream condition, one downstream condition and one wall condition. The upstream condition was set to the hydrographs in Fig. 3 for each study case. The downstream condition was set to a Neumann condition with a slope of the water surface of 0.001. The wall condition was set to free-slip; the recommended boundary condition for large scale hydrodynamic simulations in Delft3D (Deltares, 2014).



Fig. 1. Overview of the bypass reach of the Stornorrfors hydropower plant, River Umeälven, Sweden. Boxes in white correspond to the zones used in the analysis of longitudinal effects.

### 2.3. Flow scenarios

The influence of implementing flexible operating regimes on the downstream water level and depth-averaged velocity due to an increase in hydropeaking frequency was examined by, firstly, varying the hydropeaking frequency (number of flow changes per day), and secondly, varying the closing time of the spill gate. The effect of hydropeaking frequency was studied using hydrographs that corresponded to 10, 20, 30, 40, 50 and 60 flow changes per day (see Fig. 3a). This many flow changes per day is not planned within the reach, but is rather a target benchmark for a flexible future power plant (HydroFlex, 2020), so prediction of its effect is warranted. The closing time and ramp up time for these hydrographs was set to 5 min, which was the average time observed in the reach (Länsstyrelsen i Norrbotten, 2017). The effect of the spill gate closing time was studied by operating with closing times of 1, 5, 15 and 30 min (see Fig. 3b). All simulations had a sufficient spin-up time of 1 h to achieve steady state for a 50 m<sup>3</sup>/s discharge before any flow changes was applied. Following the flow change, each simulation was run sufficiently long to ensure that steady state was achieved in the entire reach for a 21 m<sup>3</sup>/s discharge.

### 2.4. Effect of flexible operating conditions on potential spawning area and ecological stranding status

#### 2.4.1. Potential spawning area

The distribution of potential spawning area was predicted based on modeled hydraulic conditions (depth and velocity) throughout

the watercourse for the six hydropeaking frequency scenarios. Optimal hydraulic conditions for spawning (see Table 1) were first obtained from the literature: optimal depth and velocity ranges for spawning of European grayling were derived from the findings of Gönczi (1989), whereas those for Atlantic salmon and brown trout were derived from those of Louhi et al. (2008). The distributions of the optimal spawning area, based on these hydraulic conditions, for the three species were then predicted across the watercourse as a function of the operating conditions using the hydrographs in Fig. 3b. The lowest extent of the water level, i.e. the low-water mark (LWM), was computed for a steady state case with a discharge of 21 m<sup>3</sup>/s. The potential spawning area that was above the LWM was then identified as potential spawning locations in risk of dewatering.

Longitudinal effects of hydropeaking frequency on potential spawning area were determined by examining differences among six representative study zones downstream of the spillway outlet (see Fig. 1). Each zone covered approximately the same distance (≈1.1–1.2 km), with placement chosen so that transitions between contiguous zones did not occur in rapids. By computing the area of the potential spawning area (Table 1) in each time step for each species, the transient effect on the local potential spawning areas in each respective zone was determined for the six hydropeaking flow scenarios (see Fig. 3a). Similarly, the area of the potential spawning areas that ran the risk of dewatering (i.e. potential spawning areas above the LWM) was computed for the six study zones for the six flow scenarios (see Fig. 3b).

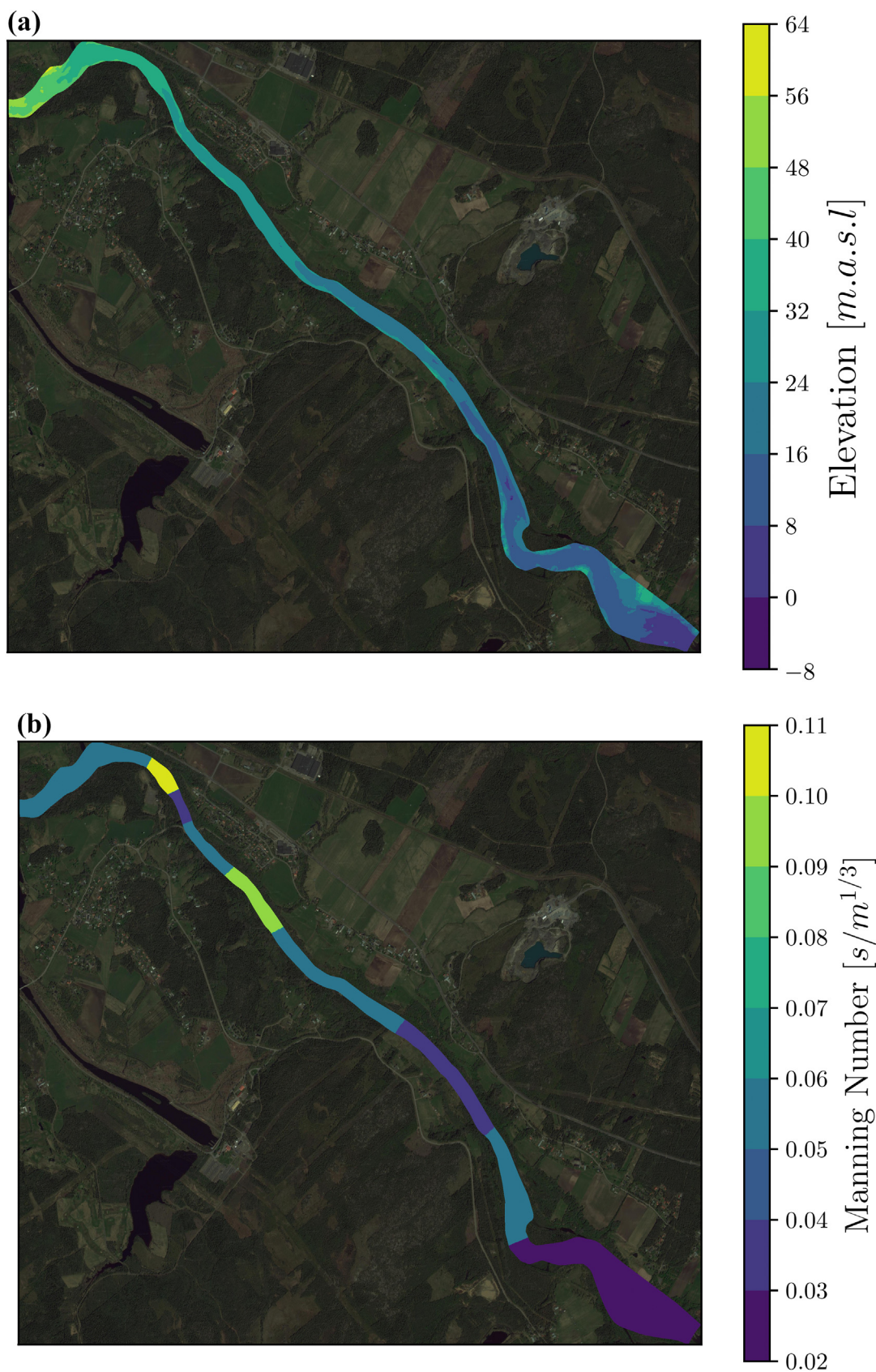
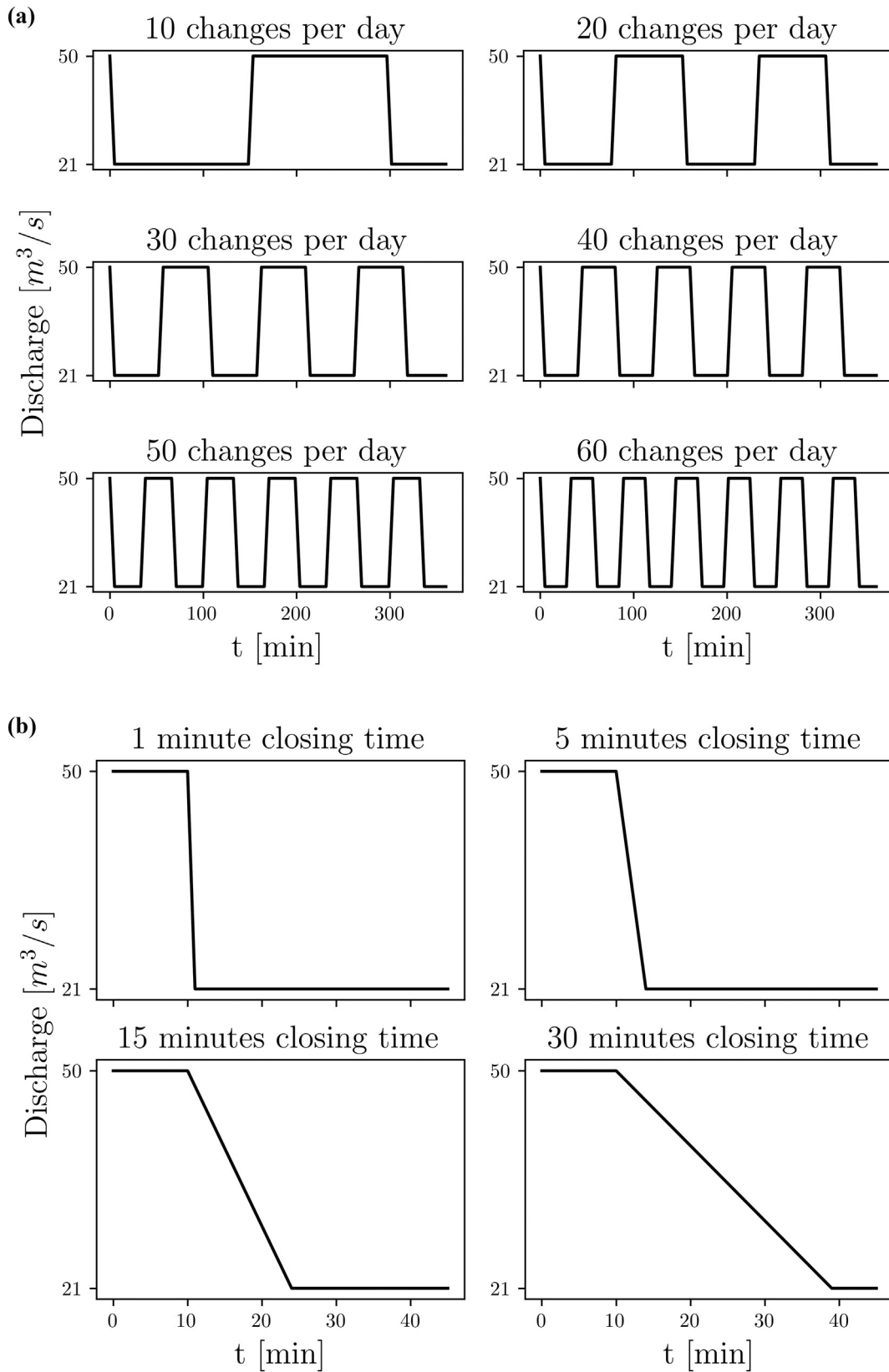


Fig. 2. (a) DEM obtained from photogrammetry measurements; (b) calibrated Manning number distribution obtained from validation with water-level measurements.



**Fig. 3.** Hydrographs used in this study: (a) hydrographs used for investigating the effect of hydropeaking frequency; (b) hydrographs used for investigating the effect of spill gate closing time.

**Table 1**  
Hydraulic conditions for potential spawning habitat and ecological stranding status.

		European grayling	Brown trout	Atlantic salmon	
Potential spawning habitat					
Optimal depth	Range [m]	0.30–0.50 <sup>a</sup>	0.20–0.30 <sup>b</sup>	0.25–0.55 <sup>b</sup>	
Optimal velocity	Range [m/s]	0.23–0.90 <sup>a</sup>	0.20–0.50 <sup>b</sup>	0.15–0.60 <sup>b</sup>	
Ecological stranding status <sup>c</sup>					
	Dewatering rate [cm/s]	Fry	Juveniles	Fry	Juveniles
Very good		<0.2	<1.0	<0.2	<1.5
Good		0.2–0.3	1.0–1.2	0.2–0.3	1.3–1.5
Moderate		0.3–0.4	1.2–2.0	0.3–0.4	3.0–4.5
Unsatisfactory		0.4–0.5	2.0–3.0	0.4–0.5	4.5–6.0
Bad		>0.5	>3.0	>0.5	>6.0

<sup>a</sup> (Gönczi, 1989).

<sup>b</sup> (Louhi et al., 2008).

<sup>c</sup> (Moreira et al., 2019).

### 2.5. Ecological stranding status

Dewatering time for each node was defined as the time from the initial decrease in water surface elevation until the time when the node had been dewatered. The decrease in water level as a function of time was approximately captured with the function

$$WSE_{fit}(t) = \begin{cases} WSE_{max} & , t < \theta \\ (WSE_{max} - WSE_{min})e^{-(t - \theta)/\tau} + WSE_{min} & , t \geq \theta \end{cases} \quad (1)$$

where  $WSE_{max}$  is the water surface elevation (WSE) before the decrease,  $WSE_{min}$  is the WSE after the decrease (or the elevation of the bathymetry in that node if the node is dewatered),  $\theta$  is a time-lag coefficient and  $\tau$  is a coefficient describing the shape of the decrease event. The curve fit for the four parameters was optimized using a least-squares approach in the Scientific Python optimize package (Scipy.org, 2020). The initial decrease was then defined as the first time where  $WSE_{fit}$  was less than  $WSE_{fit}(t=0)$ . This method allowed estimation of a dewatering time ( $t_{dewatering}$ ) both for situations when there was a near-monotonic decline in WSE with time (Fig. 4a) and for situations (typically in faster flow areas) when there was a more erratic decline in WSE with time (Fig. 4b). However, curve-fitting required at least four observations, meaning that it could not be applied to nodes where dewatering occurred over a shorter time period than 4 min (the simulation producing one observation per minute). Nodes with this condition were discarded from further analysis. The dewatering velocity was then computed as

$$u_{dewatering} = \frac{WSE_{max} - WSE_{min}}{t_{dewatering}} \quad (2)$$

When the discharge was reduced from 50 m<sup>3</sup>/s to 21 m<sup>3</sup>/s, a total of 23,849 nodes were dewatered. In each of these nodes, the resulting dewatering velocity  $u_{dewatering}$  was then compared to the thresholds in Table 1 and the resulting ecological status for the different life stages of the fish was calculated.

All locations within the watercourse were classified into a species-specific ecological stranding status based on the dewatering velocity (rate of reduction in water depth, cm/min) (see Table 1). This status represented the likelihood of fish avoiding stranding during dewatering. Ecological stranding status for juvenile grayling and juvenile brown trout were obtained from Swiss legislation core indicator “stranding thresholds” (Moreira et al., 2019). These assign an ecological status quality (very good, good, moderate, unsatisfactory and bad) that is dependent on the rate of dewatering, with higher status being associated with lower dewatering velocities.

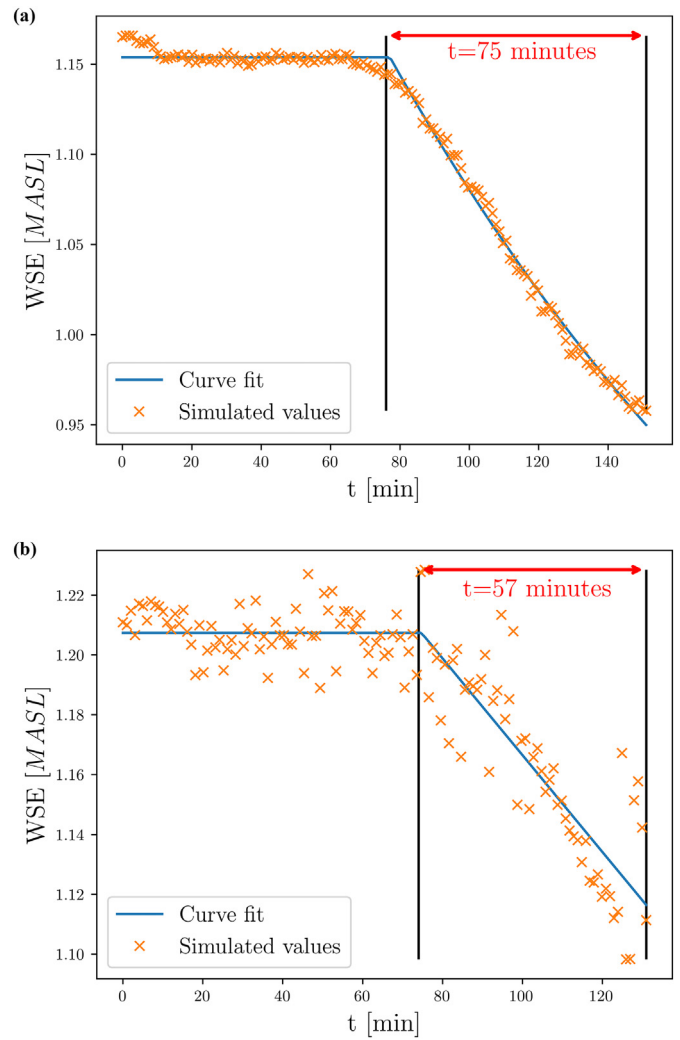


**Fig. 4.** Examples of decline in water surface elevation with corresponding curve fits: (a) near-monotonic decline; (b) erratic decline.

## 3. Results

### 3.1. Effect of hydropeaking frequency on potential spawning area

Potential spawning area for the three fish species varied in concurrence with variation in flow conditions during the hydropeaking cycle (Fig. 5a). The range of this variation was negatively related to the hydropeaking frequency. For example, a low hydropeaking frequency (10 flow changes per day) caused the potential spawning area for European grayling and Atlantic salmon to vary between 4.5 and 6.5 × 10<sup>4</sup> m<sup>2</sup>; a high hydropeaking frequency (60 flow changes per day) reduced the intra-cycle variation in potential spawning area for these species to between 4.5 and 5.5 × 10<sup>4</sup> m<sup>2</sup>. Effects were species-specific; firstly, the potential spawning area for brown trout was significantly lower than for the other two species. Secondly, the maximum potential spawning area for the different species never coincided. For example, the maximum potential spawning area for European grayling occurred several minutes after that for Atlantic salmon.

The proportion of potential spawning area that was above the LWM, and that would be dewatered at the lowest water level, was greatest for brown trout, followed by Atlantic salmon and then European grayling (see Fig. 5b). The amount of potential spawning area that was above the LWM decreased with an increase in hydropeaking frequency. A maximum of ≈40% of brown trout potential spawning area was above

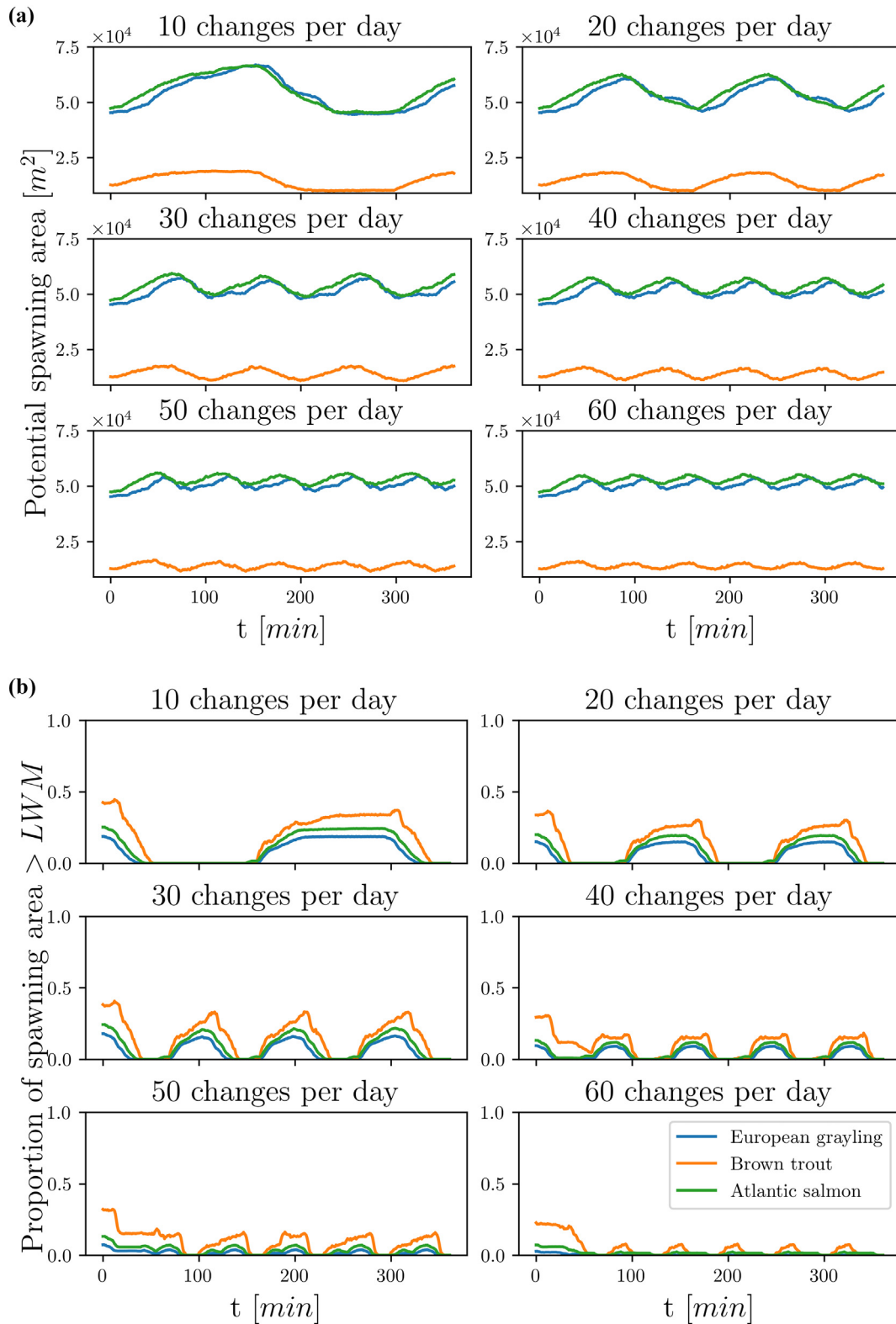
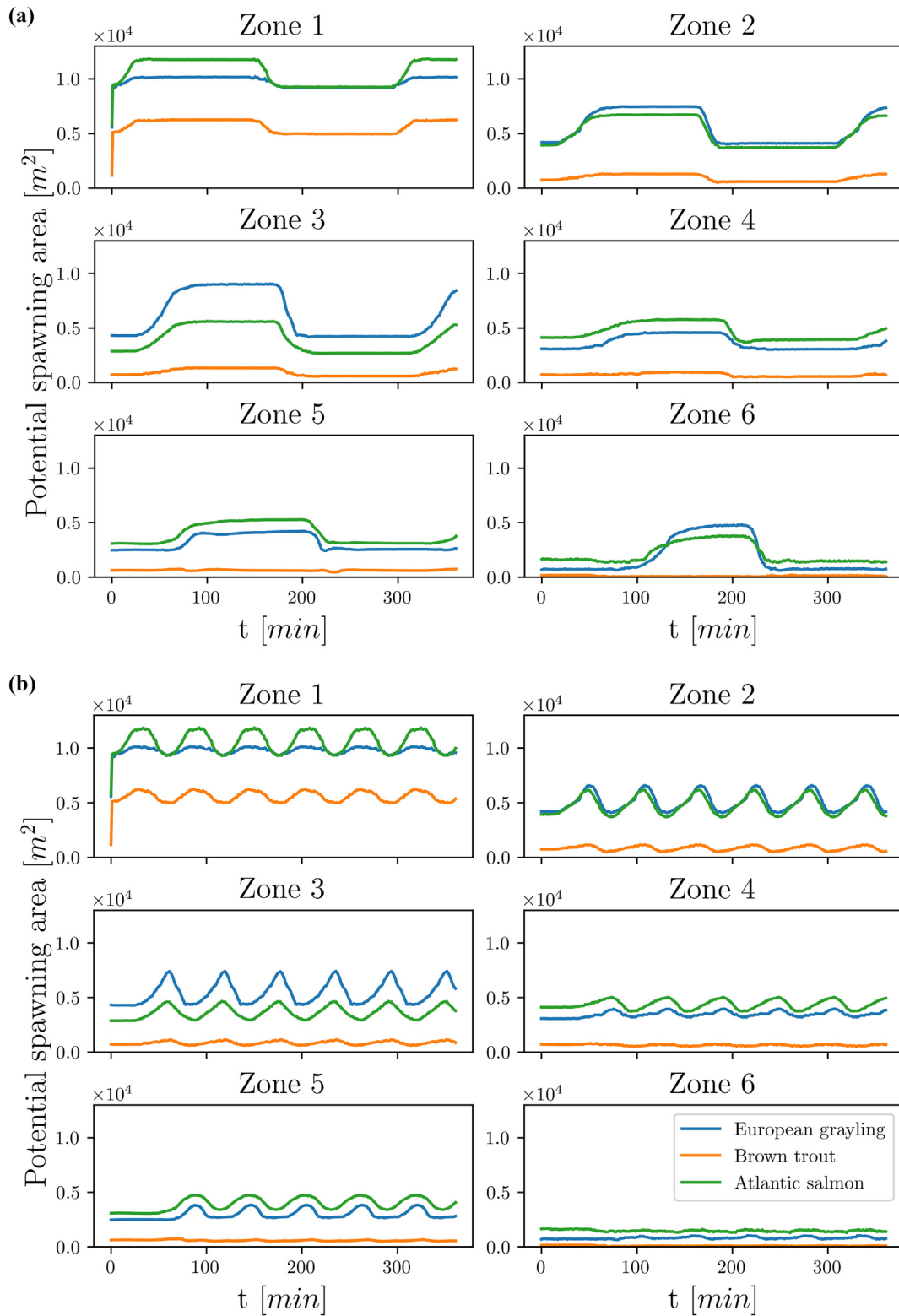


Fig. 5. Transient dynamics of the six hydropeaking scenarios: (a) potential spawning area; (b) proportion of potential spawning area above the LWM.

the LWM with 10 flow changes per day, whereas a maximum of  $\approx 25\%$  of this potential spawning area was above the LWM with 60 flow changes per day. For the simulation with 60 flow changes per day, very little European grayling or Atlantic salmon potential spawning area was above the LWM.

The dynamics of the potential spawning area strongly depended on the distance downstream from the spillway outlet (Fig. 6). The hydraulic dynamics in the study reach depended on the hydropeaking frequency (Table 2). For a frequency of 10 flow changes per day (Fig. 6a) the dynamics in the reach mainly experienced steady state conditions,



**Fig. 6.** Transient dynamics of potential spawning area in each zone: (a) hydropeaking frequency = 10 flow changes per day; (b) hydropeaking frequency = 60 flow changes per day.

associated with discharges fluctuating between 21 and 50 m<sup>3</sup>/s. When the hydropeaking frequency increased, the study reach started to exhibit a state of continuous dynamics (see Burman et al., 2020). This state of continuous dynamics, involving a sinusoidally oscillating potential spawning area, was observed for zones 2–5 for a frequency of 60 flow changes per day (Fig. 6b). The amplitude of this oscillation tended to decrease with increasing distance from the spillway outlet.

The low hydropeaking frequency scenarios that caused mainly steady state conditions tended to have more maximum potential spawning area above the LWM than the high hydropeaking frequency scenarios that caused continuous dynamics (Table 3). Longitudinal effects were also apparent. In zone 1–3 a much greater amount of potential spawning areas occurred above the LWM for a hydropeaking frequency of 10 flow changes per day (Fig. 7a) than for one of 60 flow



**Table 2**  
Potential spawning area (m<sup>2</sup>) in each zone; maximum and minimum values for the three target species for all hydropeaking scenarios.

	Potential spawning area × 10 <sup>4</sup> [m <sup>2</sup> ]	10 flow changes per day		20 flow changes per day		30 flow changes per day		40 flow changes per day		50 flow changes per day		60 flow changes per day	
		Max	Min	Max	Min	Max	Min	Max	Min	Max	Min	Max	Min
Zone 1	<i>European grayling</i>	1.01	0.91	1.01	0.91	1.01	0.91	1.01	0.91	1.01	0.91	1.01	0.96
	<i>Brown trout</i>	0.61	0.49	0.61	0.49	0.61	0.49	0.61	0.49	0.61	0.49	0.62	0.50
	<i>Atlantic salmon</i>	1.18	0.92	1.18	0.92	1.18	0.92	1.18	0.92	1.18	0.92	1.18	0.92
Zone 2	<i>European grayling</i>	0.74	0.41	0.74	0.41	0.72	0.41	0.72	0.41	0.68	0.41	0.67	0.42
	<i>Brown trout</i>	0.13	0.05	0.13	0.05	0.12	0.04	0.12	0.04	0.11	0.05	0.11	0.05
	<i>Atlantic salmon</i>	0.67	0.36	0.67	0.36	0.56	0.36	0.65	0.36	0.65	0.36	0.62	0.37
Zone 3	<i>European grayling</i>	0.89	0.42	0.89	0.42	0.86	0.41	0.83	0.43	0.80	0.43	0.74	0.43
	<i>Brown trout</i>	0.13	0.05	0.13	0.05	0.13	0.05	0.12	0.05	0.12	0.06	0.11	0.06
	<i>Atlantic salmon</i>	0.56	0.27	0.56	0.27	0.54	0.26	0.52	0.28	0.50	0.28	0.47	0.29
Zone 4	<i>European grayling</i>	0.45	0.30	0.45	0.30	0.44	0.31	0.43	0.31	0.41	0.31	0.40	0.32
	<i>Brown trout</i>	0.09	0.05	0.09	0.05	0.08	0.05	0.08	0.04	0.08	0.05	0.08	0.05
	<i>Atlantic salmon</i>	0.58	0.37	0.58	0.37	0.56	0.38	0.54	0.37	0.52	0.37	0.51	0.38
Zone 5	<i>European grayling</i>	0.42	0.25	0.40	0.25	0.40	0.25	0.40	0.25	0.38	0.26	0.38	0.27
	<i>Brown trout</i>	0.07	0.04	0.07	0.04	0.07	0.04	0.07	0.04	0.06	0.05	0.07	0.05
	<i>Atlantic salmon</i>	0.53	0.31	0.52	0.31	0.49	0.31	0.48	0.32	0.48	0.33	0.48	0.34
Zone 6	<i>European grayling</i>	0.48	0.07	0.41	0.06	0.22	0.05	0.14	0.06	0.11	0.07	0.10	0.07
	<i>Brown trout</i>	0.02	<0.01	0.02	<0.01	<0.01	<0.01	<0.01	<0.01	<0.01	<0.01	<0.01	<0.01
	<i>Atlantic salmon</i>	0.37	0.14	0.33	0.14	0.27	0.13	0.20	0.13	0.17	0.14	0.16	0.13

changes per day (Fig. 7b). In zone 1, a significant proportion of the potential spawning area appeared above the LWM in all hydropeaking scenarios except for that with 60 flow changes per day. In zone 2, there were considerable amounts of potential spawning area above the LWM for 10, 20 and 30 flow changes per day. In zone 3 there were only notable potential spawning areas above the LWM for the 10 flow changes per day case. Downstream of zone 3, hydropeaking frequency had little effect, with only negligible amounts of potential spawning area being above the LWM.

3.2. Effect of closing time on ecological stranding status

The ecological stranding status of areas that became dewatered at the LWM increased with an increase in closing time (Fig. 8). An increase in closing time from 1 min to 30 min caused a relative increase in the area that had very good ecological stranding status of 11% for European grayling and brown trout fry, 33% for European grayling juveniles, and 19% for brown trout juveniles. Ecological stranding status strongly depended on life-stage. More than 50% of the dewatered area had a bad ecological stranding status for fry, whereas more than 69% of the dewatered area had a very good status for the juvenile stage, regardless of closing time (Fig. 8). Ecological stranding status also

depended on species, with brown trout juveniles having better status than European grayling juveniles. For example, 100% of the dewatered area had a very good status for brown trout parr with a closing time of 30 min, whereas ≈93% of the dewatered area for European grayling had the same status.

Dewatered areas that experienced high dewatering velocities, indicative of a bad ecological stranding status, were found near the river banks throughout most of the watercourse. Dewatered areas that experienced lower dewatering velocities, indicative of a moderate to very good ecological stranding status, were mainly further downstream in the watercourse. A 30 min closing time caused a small increase in the dewatered area that experienced low dewatering velocity in the smaller rapids, close to the central parts of the study reach. However, closing time had little effect on ecological stranding status in the rapid Baggböleforsen section, where the inherent damping of the reach was so substantial that any sharp water level decrease was dispersed.

4. Discussion

This study has shown that hydropower operating conditions (hydropeaking frequency and spill gate closing time) have strong implications for hydraulic conditions that can sustain fishes in hydropower

**Table 3**  
Maximum potential spawning area (m<sup>2</sup>) above the LWM for the three target species for all hydropeaking scenarios. >LWM denotes the area above the low-water mark.

	Potential spawning area >LWM [m <sup>2</sup> ]	10 flow changes per day	20 flow changes per day	30 flow changes per day	40 flow changes per day	50 flow changes per day	60 flow changes per day
Zone 1	<i>European grayling</i>	2200	2200	2200	1524	502	127
	<i>Brown trout</i>	920	920	920	822	1067	5
	<i>Atlantic salmon</i>	2768	2768	2768	2077	662	239
Zone 2	<i>European grayling</i>	765	765	912	29	0	0
	<i>Brown trout</i>	502	502	527	20	7	0
	<i>Atlantic salmon</i>	1191	1191	1396	63	13	0
Zone 3	<i>European grayling</i>	536	0	112	0	0	5
	<i>Brown trout</i>	387	231	337	0	0	268
	<i>Atlantic salmon</i>	870	137	387	0	0	290
Zone 4	<i>European grayling</i>	48	0	0	0	0	0
	<i>Brown trout</i>	48	0	12	0	10	22
	<i>Atlantic salmon</i>	78	0	0	0	0	33
Zone 5	<i>European grayling</i>	0	0	0	0	0	0
	<i>Brown trout</i>	0	0	0	65	18	0
	<i>Atlantic salmon</i>	0	0	0	0	0	0
Zone 6	<i>European grayling</i>	0	0	0	0	0	0
	<i>Brown trout</i>	0	0	0	0	0	0
	<i>Atlantic salmon</i>	0	0	0	0	0	0

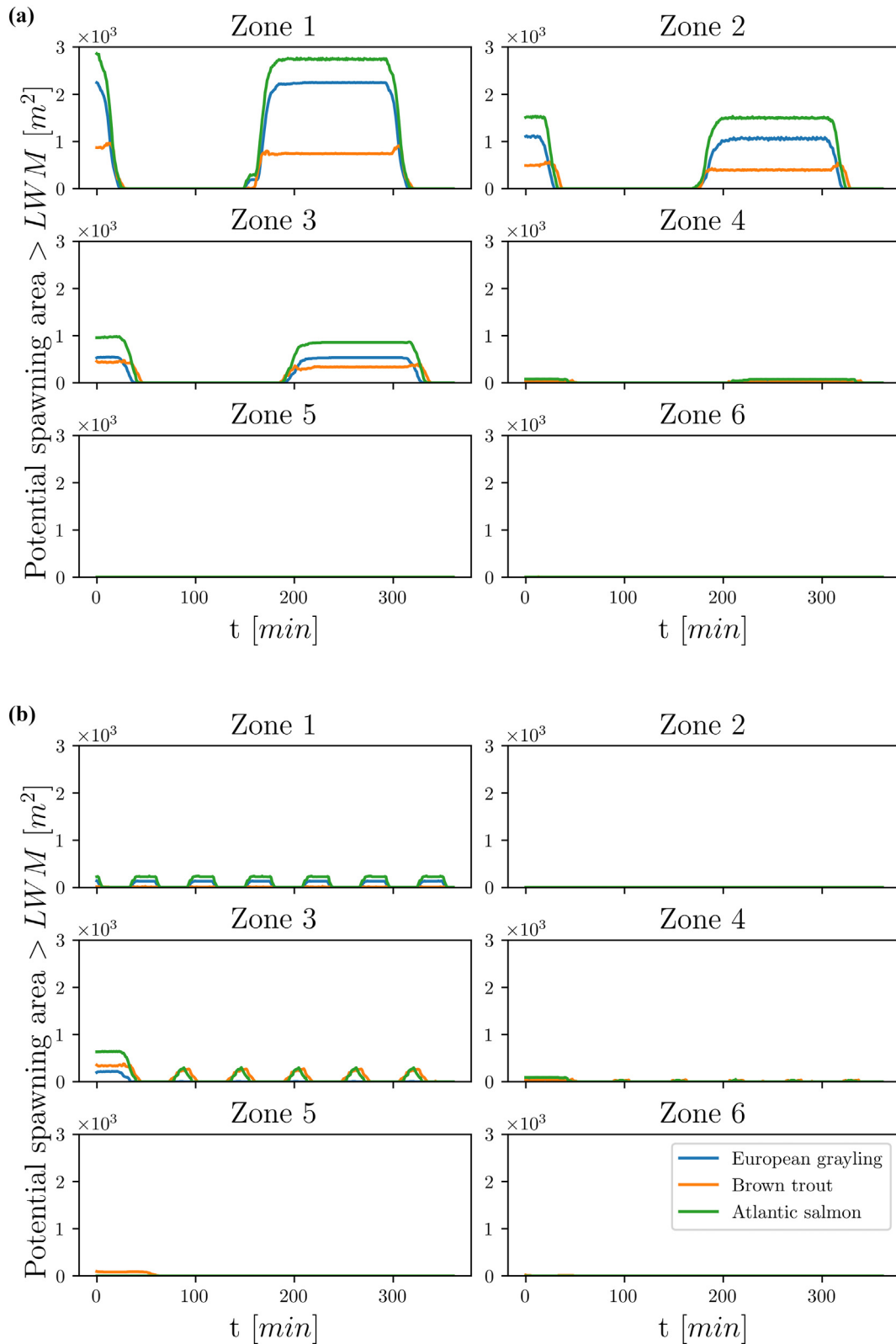


**Fig. 7.** Transient dynamics of proportion of potential spawning area above the LWM in each zone: (a) hydropeaking frequency = 10 flow changes per day; (b) hydropeaking frequency = 60 flow changes per day.

tailraces, in terms of hydraulics suitable for spawning and hydraulics suitable for avoiding stranding. In the studied reach, potential spawning area was strongly dependent on the hydropeaking frequency: an increase in hydropeaking frequency caused a reduction in variation of

potential spawning area during the hydropeaking cycle, and also caused a reduction in the amount of potential spawning area that was susceptible to dewatering during low flows. Ecological stranding status increased with an increase in spill gate closing time. Effects of changes

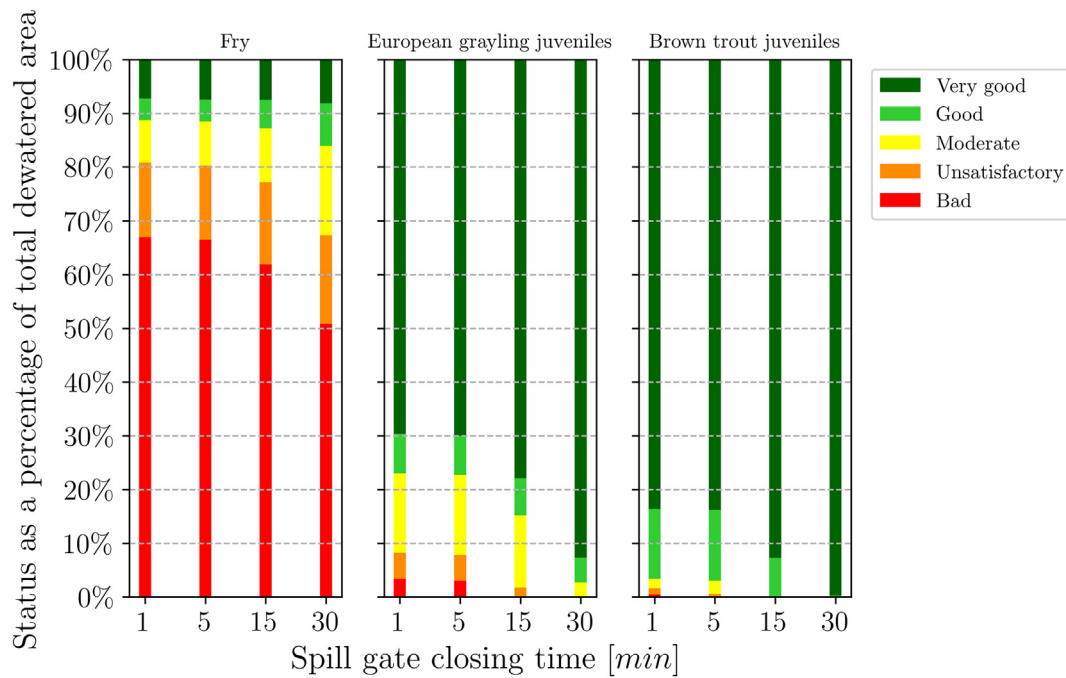


**Fig. 8.** Ecological stranding status indicator as a percentage of the total dewatered area for European grayling and brown trout fry, European grayling juveniles and brown trout juveniles for different spill gate closing times.

in operating conditions were highly dependent on distance downstream from the spillway outlet. With increasing distance downstream, there was a reduction in the proportion of the potential spawning area and there was an increase in ecological stranding status.

#### 4.1. Effect of operating conditions on potential spawning area

Potential spawning area varied temporally throughout the hydropeaking cycle, corresponding to the changing hydraulics, but the average potential spawning area and the magnitude of temporal variation decreased with an increase in hydropeaking frequency. Potential spawning area for all three species varied most when the hydropeaking frequency was lowest (10 flow changes per day), reaching a maximum for a steady state discharge of 21 m<sup>3</sup>/s and a minimum for a steady state discharge of 50 m<sup>3</sup>/s. Steady state hydraulics were less frequently observed with an increase in hydropeaking frequency, which led to a reduction in average potential spawning area and a reduction in the temporal variation in spawning area throughout the hydropeaking cycle. The reduction in potential spawning area with an increase in hydropeaking frequency suggests that flexible hydropower operating regimes, allowing for a high frequency of hydropeaking, could have negative effects on the ability of salmonids to find suitable spawning habitats by reducing the area of the river that is hydraulically suitable for spawning. Salmonids respond rapidly to changing flow conditions with regard to spawning (Vollset et al., 2016) so a low hydropeaking frequency would allow for maximum opportunity to select spawning sites when flow conditions are optimal.

Conversely, the proportion of potential spawning area that was subject to dewatering at minimum discharge decreased with an increase in hydropeaking frequency. In the low hydropeaking frequency scenarios, where steady state conditions were observed, the entire reach returned to the LWM at  $Q=21$  m<sup>3</sup>/s, causing a significant proportion of the potential spawning area to be dewatered. As the hydropeaking frequency increased, a larger proportion of the study reach exhibited continuous dynamics due to the inherent damping in the river, which in turn meant that a smaller proportion of the potential spawning area was dewatered. Flexible operating conditions with a high frequency of flow changes can therefore potentially be beneficial in terms of

providing hydraulically suitable spawning areas that are less susceptible to dewatering during low flows. Areas that may be hydraulically suitable for spawning will be less productive in terms of producing future salmonid cohorts if they are subsequently dewatered at low flows because dewatering of the spawning redds may lead to mortality of eggs and pre-emergent alevins (Becker et al., 1986; Casas-Mulet et al., 2015). It has been suggested that stable flow conditions should be maintained during spawning to minimize dewatering (Hayes et al., 2019). The modelling approach used in this study, however, suggests that very frequent flow variations can actually lead to a reduction in dewatering via initiating continuous hydrodynamics, so a very high hydropeaking frequency regime may potentially have some benefit.

The effect of dewatering of spawning redds on egg and pre-emergent alevin mortality will depend on the length for which they are dewatered as both stages show some resistance to temporary dewatering in salmonids (Becker et al., 1986). Thus the shorter dewatering period associated with a greater hydropeaking frequency may further aid the survival of egg and pre-emergent alevin stages, even if they are in (briefly) dewatered redds during short periods of low flows. The effect of hydropeaking on potential spawning area and the proportion of this area that was dewatered at low flows decreased with downstream distance from the spillway outlet. Average potential spawning area was greatest nearer to the spillway outlet (zone 1), and declined with distance downstream from the outlet. However, the proportion of potential spawning area that was dewatered at low flows was also greatest nearer to the outlet, thus suggesting the potential for dewatering of spawning redds will be greatest nearer the outlet. This dampening of hydropeaking effects with distance downstream from the source of changes in flow has been identified in previous studies (Hauer et al., 2017; Šilinis et al., 2020) but the rate of dampening depends on the watercourse properties. The advantage of the modelling approach used in the current study is that effects can be predicted in advance according to characteristics of the bypass reach.

#### 4.2. Effect of spill gate closing time on ecological stranding status

Spill gate closing time had a large effect on ecological stranding status. Increasing spill gate closing time increased ecological stranding

status for both species and both stages. Thus, our modelling results suggest that hydropeaking regimes should maximize closing time where possible. Life-stage had the largest effect on stranding status: 50% of the reach was still in the bad category for European grayling and brown trout fry for the longest spill gate closing time (30 min) whereas >90% was in the very good category for juveniles of these species. Thus, it is necessary to consider all life-stages when evaluating effects of stranding on salmonid populations. There may be situations where juveniles are relatively unaffected by stranding, but if fry are prone to stranding, negative impacts on the population may still be apparent because reduced fry abundance leads to reduced juvenile recruitment.

Ecological stranding changed longitudinally along the river, with a tendency for better ecological stranding status with increasing downstream distance from the spillway outlet. This was because of a dampening of the rate of change of water level throughout the hydropeaking cycle with increasing downstream distance, something that is consistent with previous studies (Hauer et al., 2017; Šilinis et al., 2020). In the parts of the reach where the difference between high and low water was negligible, such as along downstream riverbanks, the risk of stranding was minimal. It is likely that salmonid juveniles could be exposed to highly flexible operating conditions without stranding in the more downstream parts of the reach due to the effect of closing time on stranding being localized to areas near the outlet.

#### 4.3. Additional influences on salmonids within hydropeaked rivers

Potential spawning area was characterized in this study from hydraulic properties alone. In reality, the availability of suitable substrates plays a key role in the selection of spawning sites by salmonids (Milner et al., 2003; Louhi et al., 2008) and it is likely that the area of actual spawning habitat used by salmonids will be much smaller than that which is hydraulically suitable. However, data on substrate characteristics may not always be readily available for large river systems with high discharges, turbid waters and deep channels. In such circumstances, a modelling approach to assess potential spawning area based on hydraulic properties alone represents a simple solution to estimate the effect of hydropeaking frequency on relative changes in spawning area. In circumstances when the substrate composition has been mapped, information from predicted hydraulic properties can be integrated with substrate maps, to identify which patches of suitable substrate have satisfactory hydraulic conditions. For example, a patch of spawning gravel may be suitable for spawning in part of the watercourse far downstream from the outlet where effects of hydropeaking on hydraulics have largely dissipated but a similar patch may be unsuitable for spawning in a part of the watercourse nearer to the spillway outlet, where hydropeaking effects are greater.

The species and life-stages of the fish present have a large effect on susceptibility to stranding. In the current study reach, the stranding risk of grayling and brown trout juveniles was low regardless of closing times, and since the Atlantic salmon is less sensitive to dewatering than brown trout (Halleraker et al., 2003), it is likely that Atlantic salmon would fare better. However, species also have different risks of exposure to varying flows, related to their life-history at the earlier fry life stage. Brown trout and Atlantic salmon fry are much more dependent on the habitat and will hide in the substrate, while European grayling fry enter the water column and starts to swim earlier, making them more prone to risk of varying water flows (Auer et al., 2017). The current study used equivalent relationships for estimating stranding statuses of European grayling and brown trout, but better quantification of difference between the two species would allow better prediction of stranding effects in the bypass reach. Furthermore, it would be of interest in the future to study species other than salmonids. For example, the European river lamprey (*Lampetra fluviatilis*), a species that inhabits the study reach, is known to be negatively affected by the occurrence of

hydropower plants (Moser et al., 2002). Additionally, the circadian and seasonal behavior of the species will affect the susceptibility to stranding (Halleraker et al., 2003; Auer et al., 2017; Puffer et al., 2017). Again, better quantification of these effects would allow for better prediction in future studies.

The current study has focused on how flexible operating regimes can affect salmonid populations via influencing spawning potential and the likelihood of stranding. Hydropeaking regimes may, however, affect fish populations in other ways. The behavior of migrating salmonids is affected by hydrodynamics (Silva et al., 2020), which in turn is dependent on hydropeaking regime. Therefore, hydropeaking may affect migratory movements (Jones and Petreman, 2015; Vehanen et al., 2020). Hydropeaking may also initiate heat-stress in salmonids from associated thermopeaking (Feng et al., 2018) and increase suspended sediments (Greimel et al., 2015) which may affect fish behavior and cause direct physiological stress (Kjelland et al., 2015). The modelling approach used in the current study predicts hydraulic properties such as velocity and heat fields, so is useful for evaluating effects of hydropeaking on migration and possible heat stress. It may also be extended to give predictions on suspended sediment density in situations where there is sufficient validity data, enabling examination of turbidity effects on fishes.

## 5. Conclusions

This study shows how flexible operating conditions (hydropeaking frequency and gate closing time) can affect the potential spawning area and the stranding risk for salmonids downstream of hydropower spillways. In the watercourse studied, the potential spawning area that was susceptible to dewatering during low flows decreased with an increase in hydropeaking frequency. Very high hydropeaking frequencies, by causing a constant steady-state water level further downstream from the spillway outlet, may therefore potentially lead to less dewatering of salmonid redds. The stranding risk for fry and juveniles, however, increased with a decrease in spill gate closing time. In order for the status to be very good in the entire reach for the fry stage, the closing time would have to be longer than 30 min. Such a closing time would not be compatible with more flexible operating conditions, involving a high hydropeaking frequency. It may therefore be necessary to strike a balance in operating conditions to support salmonids at different ontological stages: ensuring that flow conditions lead to a situation where both, the dewatering of potential spawning area is minimized, and the stranding risk of juveniles is minimized. It is also necessary to consider how the effect of spillway flow conditions on potential spawning area and stranding risk change with distance downstream from the spillway. In the watercourse studied, effects of flow frequency changes were localized to the upstream part of the watercourse nearer to the spillway, whereas areas with very good ecological stranding status were found in the more downstream part of the watercourse.

## Funding

This project has received funding from the European Union's Horizon 2020 research and innovation programme under grant agreement No 764011.

## CRedit authorship contribution statement

**Anton J. Burman:** Conceptualization, Methodology, Software, Formal analysis, Investigation, Writing – original draft, Visualization. **Richard D. Hedger:** Writing – original draft, Validation, Visualization. **J. Gunnar I. Hellström:** Conceptualization, Writing – review & editing, Supervision, Resources. **Anders G. Andersson:** Conceptualization, Writing – review & editing, Supervision. **Line E. Sundt-Hansen:** Writing – original draft, Validation.

## Declaration of competing interest

The authors declare that they have no known competing financial interests or personal relationships that could have appeared to influence the work reported in this paper.

## References

- Angele, K., Andersson, A., 2018. Validation of a HEC-RAS model of the Stornorrforrs fish migration dry reach against new field data. 12th International Symposium on Ecohydraulics, Tokyo, Japan, 2018, Tokyo, Japan.
- Auer, S., Zeiringer, B., Führer, S., Tonolla, D., Schmutz, S., 2017. Effects of river bank heterogeneity and time of day on drift and stranding of juvenile european grayling (*Thymallus thymallus* L.) caused by hydropeaking. *Sci. Total Environ.* 575, 1515–1521. <https://doi.org/10.1016/j.scitotenv.2016.10.029>.
- Bakken, T.H., Forseth, T., Harby, A., Alfredsen, K., Arnekleiv, J.V., Berg, O.K., Casas-Mulet, R., Charmasson, J., Greimel, F., Halley, D., et al., 2016a. *Miljøvirkninger av effektkjøring: Kunnskapsstatus og råd til forvaltning og industri*.
- Bakken, T.H., King, T., Alfredsen, K., 2016b. Simulation of river water temperatures during various hydro-peaking regimes. *J. Appl. Water Eng. Res.* 4, 31–43. <https://doi.org/10.1080/23249676.2016.1181578>.
- Becker, C., Neitzel, D., Carlile, D., 1986. Survival data for dewatered rainbow trout (*Salmo gairdneri* rich.) eggs and alevins. *J. Appl. Ichthyol.* 2, 102–110. <https://doi.org/10.1111/j.1439-0426.1986.tb00436.x>.
- Berg, O.K., Bremset, G., Puffer, M., Hanssen, K., 2014. Selective segregation in intraspecific competition between juvenile Atlantic salmon (*Salmo salar*) and brown trout (*Salmo trutta*). *Ecol. Freshw. Fish* 23, 544–555. <https://doi.org/10.1111/eff.12107>.
- Bremset, G., Berg, O.K., 1999. Three-dimensional microhabitat use by young pool-dwelling Atlantic salmon and brown trout. *Anim. Behav.* 58, 1047–1059. <https://doi.org/10.1006/anbe.1999.1218>.
- Bremset, G., Heggenes, J., 2001. Competitive interactions in young Atlantic salmon (*Salmo salar* L.) and brown trout (*Salmo trutta* L.) in lottic environments. *Nord. J. Freshw. Res.*, 127–142. <https://doi.org/10.1111/j.1600-0633.2012.00561.x>.
- Burman, A.J., Andersson, A.G., Hellström, J.G.I., 2019. Inherent damping in a partially dry river. 38th IAHR World Congress, Panama City, September 1–6, 2019, pp. 5091–5100.
- Burman, A.J., Andersson, A.G., Hellström, J.G.I., Angele, K., 2020. Case study of transient dynamics in a bypass reach. *Water* 12, 1585. <https://doi.org/10.3390/w12061585>.
- Casas-Mulet, R., Saltveit, S.J., Alfredsen, K., 2015. The survival of Atlantic salmon (*Salmo salar*) eggs during dewatering in a river subjected to hydropeaking. *River Res. Appl.* 31, 433–446. <https://doi.org/10.1002/rra.2827>.
- Cushman-Roisin, B., Beckers, J.M., 2011. *Introduction to Geophysical Fluid Dynamics: Physical and Numerical Aspects*. Academic Press <https://doi.org/10.1016/c2009-0-00052-x>.
- Deltares, 2014. *Delft3D-Flow User Manual*.
- Deltares, 2021. *Delft 3d*. <https://oss.deltares.nl/web/delft3d> Accessed: 2021-05-21.
- Feng, M., Zolezzi, G., Pusch, M., 2018. Effects of thermopeaking on the thermal response of alpine river systems to heatwaves. *Sci. Total Environ.* 612, 1266–1275. <https://doi.org/10.1016/j.scitotenv.2017.09.042>.
- Flodmark, L., Vøllestad, L., Forseth, T., 2004. Performance of juvenile brown trout exposed to fluctuating water level and temperature. *J. Fish Biol.* 65, 460–470. <https://doi.org/10.1111/j.0022-1112.2004.00463.x>.
- Gallagher, S.P., Gard, M.F., 1999. Relationship between Chinook salmon (*Oncorhynchus tshawytscha*) redd densities and phabim-predicted habitat in the Merced and lower american rivers, California. *Can. J. Fish. Aquat. Sci.* 56, 570–577. <https://doi.org/10.1139/f98-198>.
- Gönczi, A.P., 1989. A study of physical parameters at the spawning sites of the european grayling (*Thymallus thymallus* L.). *Regul. Rivers Res. Manag.* 3, 221–224. <https://doi.org/10.1002/rrr.3450030121>.
- Greimel, F., Schülting, L., Graf, W., Bondar-Kunze, E., Auer, S., Zeiringer, B., Hauer, C., 2015. Hydropeaking impacts and mitigation. *Riverine Ecosystem Management.* 7, p. 91. [https://doi.org/10.1007/978-3-319-73250-3\\_5](https://doi.org/10.1007/978-3-319-73250-3_5).
- Halleraker, J., Saltveit, S., Harby, A., Arnekleiv, J., Fjeldstad, H.P., Kohler, B., 2003. Factors influencing stranding of wild juvenile brown trout (*Salmo trutta*) during rapid and frequent flow decreases in an artificial stream. *River Res. Appl.* 19, 589–603. <https://doi.org/10.1002/rra.752>.
- Hauer, C., Holzapfel, P., Leitner, P., Graf, W., 2017. Longitudinal assessment of hydropeaking impacts on various scales for an improved process understanding and the design of mitigation measures. *Sci. Total Environ.* 575, 1503–1514. <https://doi.org/10.1016/j.scitotenv.2016.10.031>.
- Hayes, D.S., Moreira, M., Boavida, I., Haslauer, M., Unfer, G., Zeiringer, B., Greimel, F., Auer, S., Ferreira, T., Schmutz, S., 2019. Life stage-specific hydropeaking flow rules. *Sustainability* 11, 1547. <https://doi.org/10.3390/su11061547>.
- HydroFlex, 2020. *Hydropower in climate change mitigation and adaptation*. <https://www.h2020hydroflex.eu/about/background/> Accessed: 2020-09-29.
- Jones, N., Petreman, I., 2015. Environmental influences on fish migration in a hydropeaking river. *River Res. Appl.* 31, 1109–1118. <https://doi.org/10.1002/rra.2810>.
- Kjelland, M.E., Woodley, C.M., Swannack, T.M., Smith, D.L., 2015. A review of the potential effects of suspended sediment on fishes: potential dredging-related physiological, behavioral, and transgenerational implications. *Environ. Syst. Decis.* 35, 334–350. <https://doi.org/10.1007/s10669-015-9557-2>.
- Länsstyrelsen i Norrbotten, 2017. *Tappningsschema gamla älvfåran Stornorrforrs 2017* (diarienummer 532-15339-15).
- Louhi, P., Mäki-Petäys, A., Erkinaro, J., 2008. Spawning habitat of Atlantic salmon and brown trout: general criteria and intragravel factors. *River Res. Appl.* 24, 330–339. <https://doi.org/10.1002/rra.1072>.
- McKinney, T., Speas, D.W., Rogers, R.S., Persons, W.R., 2001. *Rainbow trout in a regulated river below Glen Canyon dam, Arizona, following increased minimum flows and reduced discharge variability*. *N. Am. J. Fish Manag.* 21, 216–222 (doi:10.1577/1548-8675(2001)021%3C0216:rtiarr%3E2.0.co;2).
- Milner, N., Elliott, J., Armstrong, J., Gardiner, R., Welton, J., Ladle, M., 2003. The natural control of salmon and trout populations in streams. *Fish. Res.* 62, 111–125. [https://doi.org/10.1016/s0165-7836\(02\)00157-1](https://doi.org/10.1016/s0165-7836(02)00157-1).
- Mohammed-Ali, W., Mendoza, C., Holmes, R.R., 2020. Riverbank stability assessment during hydro-peak flow events: the lower Osage river case (Missouri, USA). *Int. J. River Basin Manag.*, 1–9. <https://doi.org/10.1080/15715124.2020.1738446>.
- Moir, H., Gibbins, C.N., Soulsby, C., Youngson, A., 2005. Phabssim modelling of Atlantic salmon spawning habitat in an upland stream: testing the influence of habitat suitability indices on model output. *River Res. Appl.* 21, 1021–1034. <https://doi.org/10.1002/rra.869>.
- Moreira, M., Hayes, D.S., Boavida, I., Schletterer, M., Schmutz, S., Pinheiro, A., 2019. Ecologically-based criteria for hydropeaking mitigation: a review. *Sci. Total Environ.* 657, 1508–1522. <https://doi.org/10.1016/j.scitotenv.2018.12.107>.
- Moser, M.L., Ocker, P.A., Stuehnenberg, L.C., Bjornn, T.C., 2002. *Passage efficiency of adult pacific lampreys at hydropower dams on the lower Columbia river, USA*. *Trans. Am. Fish. Soc.* 131, 956–965.
- Puffer, M., Berg, O.K., Einum, S., Saltveit, S.J., Forseth, T., 2017. Energetic consequences of stranding of juvenile Atlantic salmon (*Salmo salar* L.). *J. Water Resour. Protect.*, 163–182. <https://doi.org/10.4236/jwrp.2017.92012>.
- Saltveit, S., Halleraker, J., Arnekleiv, J., Harby, A., 2001. Field experiments on stranding in juvenile Atlantic salmon (*Salmo salar*) and brown trout (*Salmo trutta*) during rapid flow decreases caused by hydropeaking. *Regul. Rivers Res. Manag.* 17, 609–622. <https://doi.org/10.1002/rrr.652>.
- Saltveit, S.J., Brabrand, Å., Juárez, A., Stickler, M., Dønnum, B.O., 2020. The impact of hydropeaking on juvenile brown trout (*Salmo trutta*) in a norwegian regulated river. *Sustainability* 12, 8670. <https://doi.org/10.3390/su12208670>.
- Scipy.org, 2020. *Scipy*. <https://docs.scipy.org/doc/scipy/reference/tutorial/optimize.html> Accessed: 2020-07-10.
- Šilinis, L., Punys, P., Radzevičius, A., Kasiulis, E., Dumbrasukas, A., Jurevičius, L., 2020. An assessment of hydropeaking metrics of a large-sized hydropower plant operating in a lowland river, Lithuania. *Water* 12, 1404. <https://doi.org/10.3390/w12051404>.
- Silva, A.T., Bærum, K.M., Hedger, R.D., Baktoft, H., Fjeldstad, H.P., Gjelland, K.Ø., Økland, F., Forseth, T., 2020. The effects of hydrodynamics on the three-dimensional downstream migratory movement of Atlantic salmon. *Sci. Total Environ.* 705, 135773. <https://doi.org/10.1016/j.scitotenv.2019.135773>.
- UNFCCC, 2016. *The Paris agreement*. <https://unfccc.int/process-and-meetings/the-paris-agreement/the-paris-agreement>.
- Vattenfall, 2020. *Stornorrforrs*. <https://powerplants.vattenfall.com/sv/stornorrforrs> Accessed: 2020-07-06.
- Vehanen, T., Louhi, P., Huusko, A., Mäki-Petäys, A., van der Meer, O., Orell, P., Huusko, R., Jaukkuri, M., Sutela, T., 2020. Behaviour of upstream migrating adult salmon (*Salmo salar* L.) in the tailrace channels of hydropeaking hydropower plants. *Fish. Manag. Ecol.* 27, 41–51. <https://doi.org/10.1111/fme.12383>.
- Vericat, D., Ville, F., Palau-lbars, A., Batalla, R.J., 2020. Effects of hydropeaking on bed mobility: evidence from a pyrenean river. *Water* 12, 178. <https://doi.org/10.3390/w12010178>.
- Vollset, K., Skoglund, H., Wiers, T., Barlaup, B., 2016. Effects of hydropeaking on the spawning behaviour of Atlantic salmon *Salmo salar* and brown trout *Salmo trutta*. *J. Fish Biol.* 88, 2236–2250. <https://doi.org/10.1111/jfb.12985>.